Laser Energy Monitor for Double-Pulsed 2-μm IPDA Lidar Application

Tamer F. Refaat[a], Mulugeta Petros[b], Ruben Remus[b], Jirong Yu[b] and Upendra N. Singh[b]
[a]Applied Research Center, Old Dominion University, 12050 Jefferson Ave., Newport News, VA USA 23606; [b]NASA Langley Research Center, 11 Langley Blvd., Hampton, VA USA 23681

ABSTRACT

Integrated path differential absorption (IPDA) lidar is a remote sensing technique for monitoring different atmospheric species. The technique relies on wavelength differentiation between strong and weak absorbing features normalized to the transmitted energy. 2-μm double-pulsed IPDA lidar is best suited for atmospheric carbon dioxide measurements. In such case, the transmitter produces two successive laser pulses separated by short interval (200 μs), with low repetition rate (10Hz). Conventional laser energy monitors, based on thermal detectors, are suitable for low repetition rate single pulse lasers. Due to the short pulse interval in double-pulsed lasers, thermal energy monitors underestimate the total transmitted energy. This leads to measurement biases and errors in double-pulsed IPDA technique.

The design and calibration of a 2-μm double-pulse laser energy monitor is presented. The design is based on a high-speed, extended range InGaAs pin quantum detectors suitable for separating the two pulse events. Pulse integration is applied for converting the detected pulse power into energy. Results are compared to a photo-electro-magnetic (PEM) detector for impulse response verification. Calibration included comparing the three detection technologies in single-pulsed mode, then comparing the pin and PEM detectors in double-pulsed mode. Energy monitor linearity will be addressed.

Keywords: Laser energy monitor, Double-pulsed laser, IPDA lidar, Integrated-path differential absorption lidar, Carbon dioxide, Pulse detection

1. INTRODUCTION

Remote sensing using the integrated path differential absorption (IPDA) lidar is suitable for monitoring different atmospheric trace gases [1-4]. Similar to the differential absorption lidar (DIAL), the technique relies on the differentiation between strong and weak absorbing features of the gas to be monitored with respect to wavelength. Unlike DIAL, IPDA depends on hard target return signals that are proportional to the gas content throughout the whole range, or column, after normalization to the transmitted laser energy. Therefore, IPDA is a special case of DIAL, were the range cell is defined for the whole range. The loss of the range-resolved profiling sensitivity that is provided through conventional DIAL is a limitation of IPDA technique. On the other hand, relying on hard target and laser energy monitor strong signals provides high signal-to-noise ratio (SNR) which contributes significantly to the measurement sensitivity and accuracy of the IPDA technique [1-4].

IPDA lidar systems operating at the 2-μm wavelength are best suited for monitoring atmospheric carbon dioxide (CO_2) [5-6]. This is due to the existence of several strong absorption features of the gas in this wavelength. Recently, a double-pulse 2-μm IPDA lidar system have been integrated and evaluated at NASA Langley Research Center (LaRC) [5-6]. In this system, the transmitter produces two successive laser pulses separated by 200 μs interval, with 10 Hz repetition rate. The wavelengths of the transmitted pulses are tuned to strong and weak CO_2 absorption around the R30 line, namely the on-line and off-line, respectively. The short interval between the on-line and off-line pulses reduces atmospheric biases in the CO_2 measurement. Besides, the technological capability of producing both pulses using a single pulse from the pump laser raises the transmitter operating efficiency [7]. In this double-pulsed CO_2 IPDA system extended range InGaAs pin photodetector is used for measuring the hard target return signal. Thorough investigation was conducted for monitoring the transmitted laser energy to apply the correct power normalization for the CO_2 optical depth calculation.

Conventional commercial pulsed laser energy monitors relies on thermal detectors. Thermal detectors, such as pyroelectric, inherently integrate the input radiation power to produce an output signal that is proportional to pulse energy. In the pyroelectric detector the radiation pulse (from laser) is absorbed by the surface of the detector resulting in

increasing its temperature. This causes a temperature change to the pyroelectric material attached to the absorber resulting in local polarization through electric charge separation within the crystal. This translates to an electric signal, that decays slowly (thermal time constant) through cooling the element by sinking out the heat. The electric signal is usually buffered through a field-effect transistor (FET). The FET also serves in blocking the charges, generated in the pyroelectric equivalent capacitance, through its high input impedance (electrical time constant). Thermal detectors have the sensitivity and dynamic range suitable for directly measuring pulsed lasers energy without strong wavelength dependence, but they are slow due to the thermal time constant (i.e., the device has to completely cool down from the first pulse in order to detect a second pulse), which limits their operating frequency [8-9]. Thus, due to the short pulse interval in double-pulsed lasers, thermal energy monitors underestimate the total pulse-pair transmitted energy.

Quantum detectors provide electrical signals proportional to the optical radiation power (photon energy per time). Therefore, for monitoring laser pulse energy, the detector output has to be integrated with respect to time, which results in extending the collected data per shot relative to thermal detectors. Nevertheless, quantum detectors exhibit high bandwidth sufficient to distinguish the double-pulse event of the 2-μm laser. Among quantum detectors, photodiodes with pin structure are suitable for ultrafast photo-detection. By introducing an undoped intrinsic region sandwiched between p and n regions of a conventional pn photodiode, the device capacitance is reduced resulting in higher bandwidth with high quantum efficiency. The capacitance can be feather reduced by reverse biasing the device [8]. Higher bandwidth could be achieved using photo-electromagnetic (PEM) detectors but with lower sensitivity. A PEM detector relies on deflecting the trajectory of the photo-generated charge carriers by introducing a magnetic field along the semiconductor using a permanent magnet. PEM detectors exhibit low impedance without external bias voltage requirement, suitable for direct coupling to 50 Ω loads without the need for external amplification. Yet, the longer charge carrier trajectory results in higher noise and lower device sensitivity [8].

In this paper, the design and calibration of a 2-μm double-pulse laser energy monitor is presented. The design is based on a high-speed, extended range InGaAs pin quantum detectors suitable for separating the two pulse events. Results of the pin detector (PIN) are compared to a PEM detector for impulse response verification. Calibration included comparing the energy read-out of the three detection technologies in single-pulsed mode, where the operating conditions meet the thermal detector specifications. Then, both PIN and PEM detectors operation was compared for the double-pulsed mode. This results in defining the energy monitor transfer characteristics including linearity.

2. LASER ENERGY MONITOR SETUP

Figure 1 shows a schematic of the 2-μm double-pulsed laser energy monitor setup. Two steering mirrors, M1 and M2 direct the laser output to a 6× beam expander formed by X1 and X2 mirrors. The 21.4 mm expanded beam is then focused using a parabolic mirror, X3, onto a calibrated pyroelectric thermal detector, D1 (Gentec-eo; QE25SP-S-MT) [9]. This allows D1 to measure the whole transmitted energy during the energy monitor calibration. Since M1 has 99% 2-μm reflectivity, radiation leak is directed to an integrating sphere through a neutral density filter, NDF, by 1% AR coated beam splitter, M3. An extended range, 300 μm diameter, PIN detector (Hamamatsu; G8423-03), D2, is mounted on the integrated sphere. Optical radiation incident on D2 through M1, M3, NDF and the sphere was set to insure beam uniformity and avoid saturation. Similarly, part of the 1% scattered radiation out of M2 is detected by a PEM detector (VIGO System; PEM-L 10.6), D3. D1 energy readings were collected through an energy readout instrument (Gentec-eo; MAESTRO) that interfaces the data to a digital recorder [9]. This produces a single readout per laser pulse. Simultaneously, D2 and D3 signals were digitized and recorded using two-channel, 10-bit analog-to-digital converter card (Agilent; U1065A, DC252) at 500MS/s rate (2 ns sampling time). This produces two profiles for every laser pulse each consists of 3000 sample record length (6 μs). DC coupling of D2 to the digitizer was conducted through a trans-impedance amplifier (FEMTO; DHPCA-100), set to a gain of 10^3 V/A with 80 MHz full bandwidth. D3 was connected directly to the digitizer 50 Ω input. The synchronization of the detectors records was achieved through the laser Q-switch trigger signal. During the IPDA lidar normal operation X3 and D1 are removed and the expanded beam is transmitted toward a hard target. All other components are integrated within the 2-μm laser enclosure. D2 is similar to the IPDA science channels detectors used to measure the hard target return, but without the temperature control option. For calibrating the integrated laser energy monitor, the 2-μm laser was operated in a single-pulse mode. This allows energy calibration transfer from D1 to D2 and D3. Then, the laser was operated in double-pulse mode for separate on-line and off-line pulse energy detection verification through the correlation between D2 and D3 readouts.

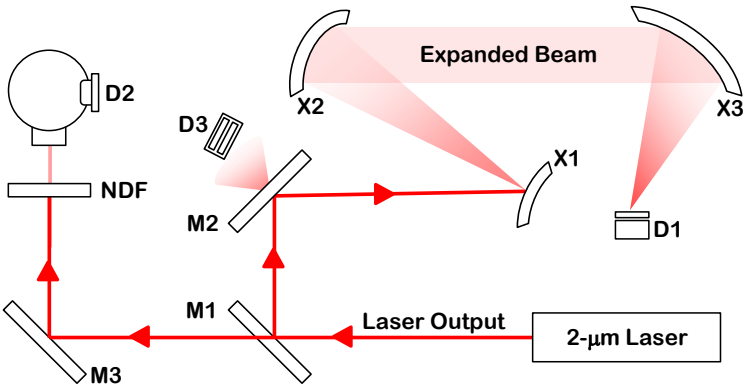

Figure 1. Setup of the 2-µm, double-pulsed laser energy monitor. The setup is integrated in the laser packaging up to X2. Mirror X3 and thermal detector D1 are installed outside the laser package for energy monitor testing and removed during IPDA normal operation.

3. CALIBRATION TRANSFER THROUGH SINGLE-PULSE OPERATION

Depending on the Q-switch triggering scheme, the 2-µm laser can produce either a single-pulse or double-pulse output, using a single pulse from a 792 nm pump laser diodes. The output of the 2-µm laser energy can be controlled by changing the pump laser diode current [7]. D1 is capable to operate with a maximum laser pulse repetition rate of 6 kHz. Operating the 2-µm laser in single-pulse mode, at 10 Hz repetition rate, allows precise reading from D1 with sufficient settling time (100 ms) to overcome the detector thermal time constant. Single-shot energies were recorded for each laser pulse as shown in figure 2a. By setting the pump diodes current with 2 A incremental steps, the process is repeated for different pump laser energy levels. 1000 shots were collected at each level as shown in the figure. Figure 2b shows the average laser energy, E (in mJ), versus the pump laser energy, E_p (in J), setting. Applying a polynomial fit to the data results in a quadratic fit in the form

$$E = -29.78 \cdot E_p^2 + 261.31 \cdot E_p - 451.42 \quad (1)$$

The inset of figure 2b shows the linear relation between the pump diodes current and the resultant pump energy. Simultaneously, both the PIN and PEM detectors are monitoring the laser energy. For each data point of figure 2a a

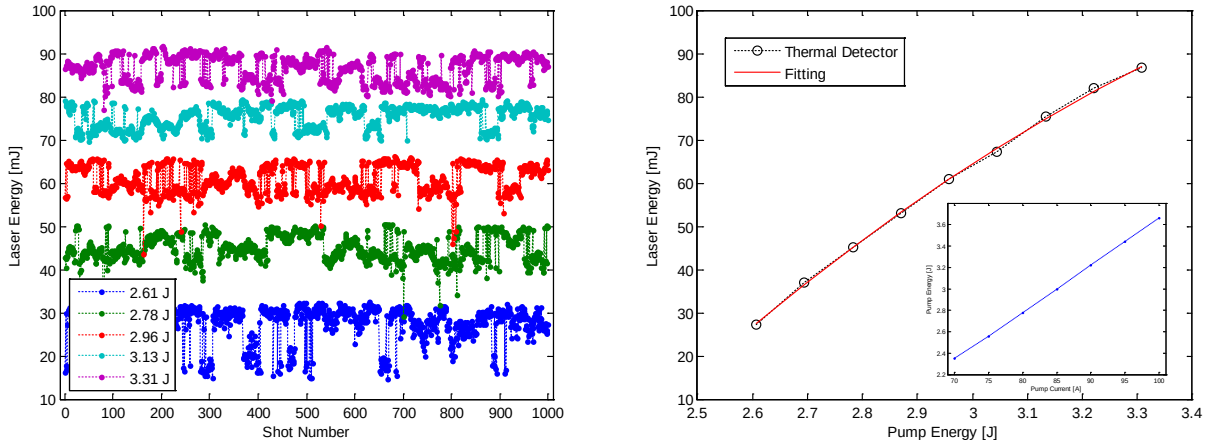

(a) (b)

Figure 2. (a) Per-shot laser energy measurements using the calibrated thermal detector at different pump laser energy levels. (b) Curve fitting of 1000 shot average laser energy versus laser current.

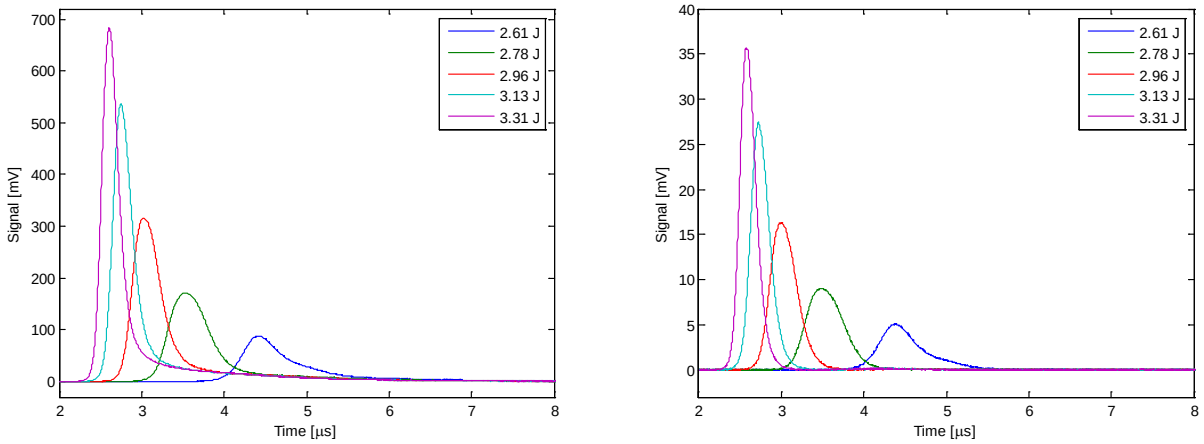

(a) (b)

Figure 3. (a) PIN and (b) PEM quantum detectors pulsed output signals at different laser current levels corresponding to different laser energy. Each waveform is an average of 1000 pulses after background subtraction.

pulse is generated from either detector. Figure 3a and 3b show the averaged pulse profile measured by the PIN and PEM detectors, respectively, at selected energy levels. Inverse relation is observed between pulse-width and energy. Higher pump energy requires shorter circulating time in the laser cavity for the 2-μm pulse to build-up. The PEM detector exhibit faster pulse response, with 1 ns time constant equivalent to 160 MHz, with a small undershoot. The PIN detector suffers longer settling time due bandwidth limitation of the detector and trans-impedance amplifier combination (60 and 80 MHz, respectively).

Pulse integration for both the PIN and PEM detectors was performed, per-shot, using the trapezoid rule after subtraction the background signal. The background is defined as the mean signal between 1 and 2.2 μs (samples 500 and 1100). The integration was conducted with fixed limits between 2 and 9.6μs (samples 1000 and 4800). Figure 4a shows the pulse integration mean versus the mean laser energy for the different pump energy levels, for both PIN and PEM detectors. Polynomial curve fitting was conducted between the laser energy and the pulse integral resulting in the relations

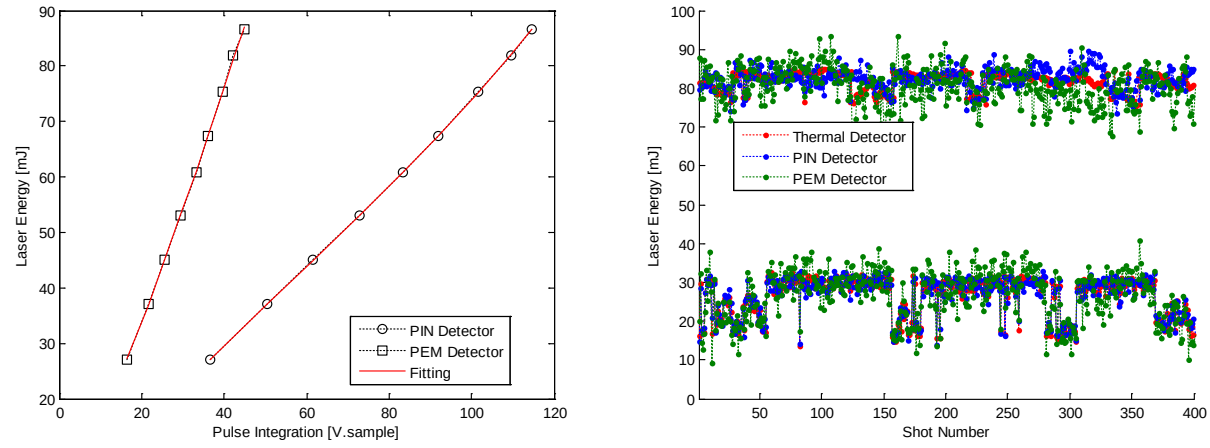

(a) (b)

Figure 4. (a) PIN and PEM quantum detectors pulse-integration calibration to the output laser energy. PEM pulse integration is multiplied by a factor of 10 for clarity. (b) Appling the PIN and PEM detectors calibration to calculate the single-shot laser energy, shown only for 2.61 and 3.22 J pump energies.

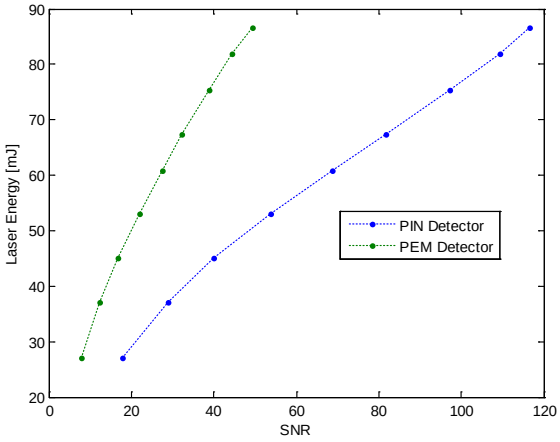

Figure 5. PIN and PEM detectors SNR versus laser energy. SNR was calculated using 1000-shot average of single-shots SNR. Single-shot SNR is calculated by dividing the peak-to-peak pulsed signal to the standard deviation of the background.

$$E = 9.543\times10^{-8}\cdot I_{PIN}^{4} - 1.055\times10^{-5}\cdot I_{PIN}^{3} + 1.367\times10^{-5}\cdot I_{PIN}^{2} + 0.748\cdot I_{PIN} \quad (2)$$

and

$$E = -8.186\times10^{-2}\cdot I_{PEM}^{4} + 0.672\cdot I_{PEM}^{3} - 0.681\cdot I_{PEM}^{2} + 16.262\cdot I_{PEM} \quad (3)$$

for the energy calibration using the PIN and PEM detectors, respectively, where I_{PIN} and I_{PEM} are their pulse integral (in Volt×sample). Applying equations (2) and (3) to the values of the integrated pulses, per shot, correlates to the laser energy measured by the thermal detector as shown in figure 4b. For the data presented in this figure, the correlation coefficients between the thermal and the PIN detectors are 0.9528 and 0.4624 for 2.61 and 3.22 J pump energy, respectively. The same coefficients between the thermal and the PEM detectors are 0.8178 and 0.5489 for the same pump energies. This indicates that both quantum detectors correlate better to the thermal detector at lower laser energy, with better correlation from the PEM at higher energy. Figure 5 shows the SNR versus the output laser energy. SNR is calculated by dividing the pulse peak-to-peak value to the standard deviation of the background signal, per shot, then averaged for each energy level. SNR is proportional to the laser energy with the PIN detector exhibiting higher SNR compared to the PEM.

4. DOUBLE-PULSE OPERATION

As discussed earlier, thermal detectors are characterized with long settling time. Figure 6 compares the calibrated thermal detector response to single and double-pulsed laser. In single-pulse operation with low repetition rate (10 Hz), time between successive pulse events is sufficient for recovering the detector impulse response (≈5 ms). In such case, the detected peak voltage is proportional to the incident pulse radiation energy. In double-pulse operation, time separation between the two pulse events is much shorter than the detector settling time. As a result, the detected peak voltage at the detector output would still be proportional to, but underestimating, the total energy of both pulses. Separating the on-line and off-line energies from the thermal detector output is difficult. Therefore, the thermal energy monitor cannot read the individual energy of each pulse, which is a main requirement for the IPDA lidar technique.

Usually, quantum detectors bandwidth (>10MHz) is sufficient for distinguishing the power profile of each pulse as illustrated in figure 7 for the PIN detector. By separating the on-line and off line pulse response, each can be integrated separately. Then the integration is correlated to the energy, using equation (2) or (3) depending on the detector used. This is illustrated in figure 8a, which compares the PIN and PEM detectors energy measurement for the on-line and off-line pulses during double-pulse operation. Correlation coefficient calculation, between the PIN and PEM on-line and off-line energies, per-shot, results in 0.1451 and 0.5249, respectively. Although high correlation between the lower off-line energies is observed, the higher on-line energy correlation indicates some near-saturation possibility. Adding the on-line

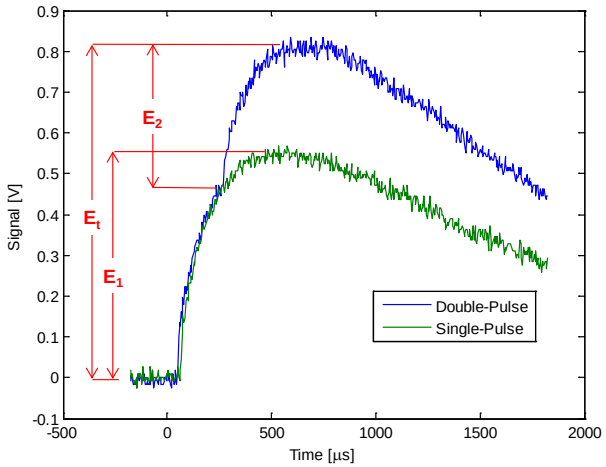

Figure 6. Comparing the impulse response of the thermal detector to single-pulsed and double-pulsed lasers. Due to long settling time, the detector underestimates the total energy of the two pulses (i.e., $E_t < E_1 + E_2$).

and off-line energies, per shot, for both detectors results in the total energy generated per pump pulse. Figure 8b compares the total energy obtained from the PIN and PEM detectors measurement to the thermal detector reading. The figure confirms the thermal detector total energy underestimation, with close PIN and PEM results. The 1000 shot averaged energies is compared in figure 9a for three different pump energies. The figure indicates the close energy measurement between the PIN and PEM detector, with 0.9843 and 0.9992 correlation coefficients for the on-line and off-line mean energies respectively. Figure 9b presents the SNR obtained from these data, calculated as discussed earlier. PIN detector results in higher SNR than the PEM detector. This attributed to the higher noise contents of the PEM detector due to the longer charge carrier trajectory presented by the magnetic field, as discussed earlier. For both detectors, on-line SNR is higher than the off-line due to the higher on-line transmitted energy.

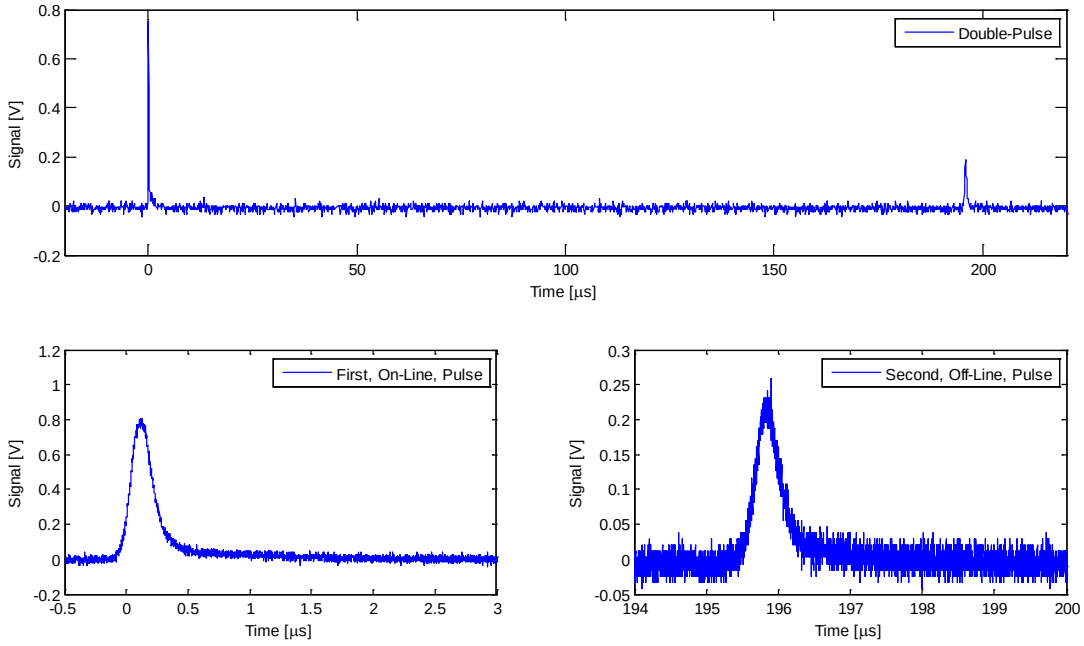

Figure 7. PIN detector pulse response to double-pulsed laser. High detection bandwidth results in a short settling time, sufficient to distinguish both pulse events, suitable for monitoring their energy separately. The 2-µm IPDA was set to transmit higher on-line energy than off-line.

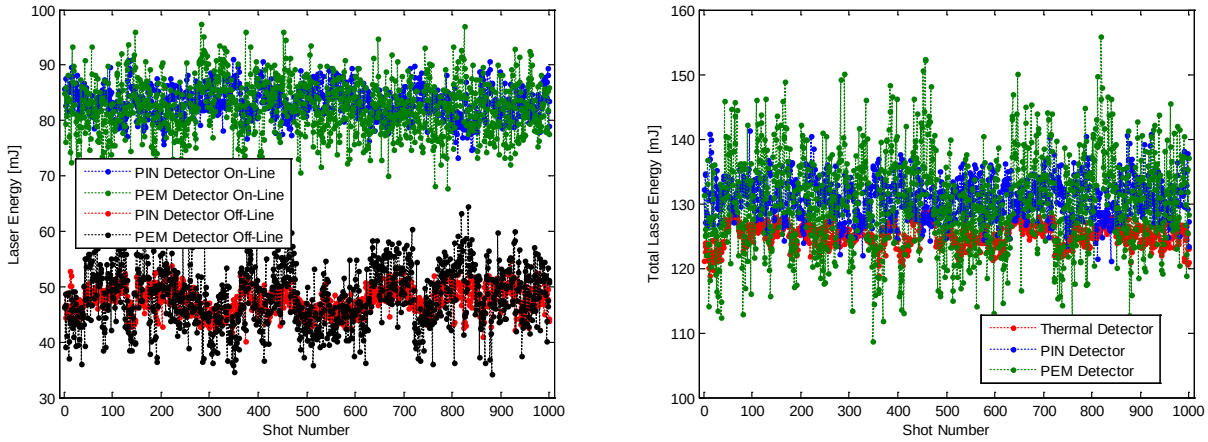

(a) (b)

Figure 8. Double-pulsing results for 3.05 J pump energy per-shot. (a) Comparing the PIN and PEM detectors output integration for the on-line and off-line energy measurement. (b) Total energy measurement, obtained by adding the on-line and off-line energies, presented in (a) for the PIN and PEM detectors as compared to the thermal detector total energy measurement.

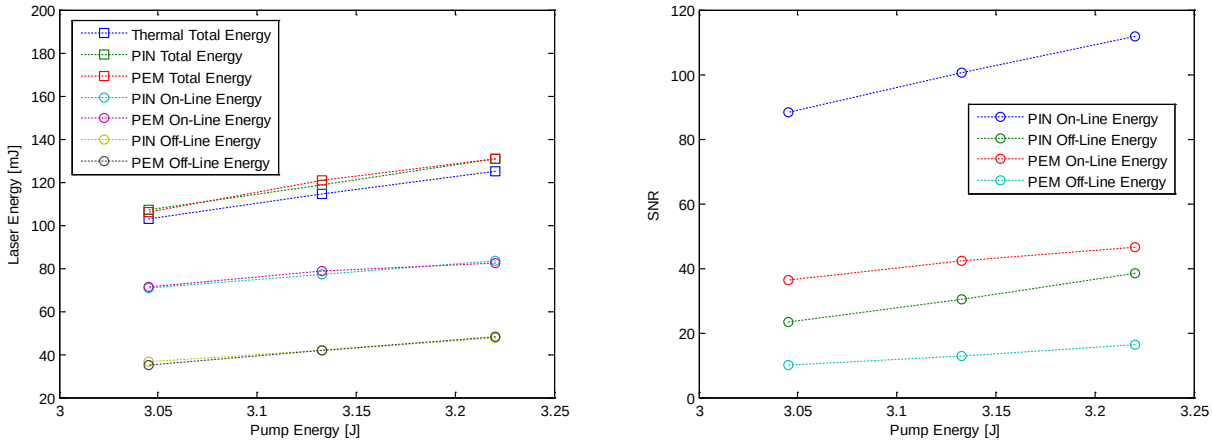

(a) (b)

Figure 9. (a) Comparing the 1000 shot mean energy measurement obtained by the three detectors. (b) Corresponding on-line and off-line SNR for the PIN and PEM detectors.

5. SUMMARY AND CONCLUSIONS

IPDA lidar is a promising remote sensing technique for measuring atmospheric trace gases. Double-pulse IPDA lidar operating at the 2-μm wavelength is suited for measuring atmospheric CO_2. Optical depth is the main IPDA product, which is obtained through normalizing the hard target return signals to the energies of the transmitted laser pulses. This requires accurate measurement of the transmitted laser pulses energies, simultaneously while operating the instrument. Energy monitors relying on thermal detectors are suitable for measuring the laser pulse energy. Nevertheless, thermal detectors suffer from long settling time insufficient to distinguish the on-line and off-line energies for double-pulse transmitters. Quantum detectors exhibit shorter settling time that is suitable for this application but produce a power proportional output rather than energy. Therefore, quantum detectors output have to be integrated to correlate to the transmitted energy.

Extended range InGaAs pin (PIN) and photo-electromagnetic (PEM) quantum detectors were investigated for the 2-μm CO_2 IPDA lidar. Both detectors were installed inside the laser enclosure. Both detectors were calibrated with respect to the laser transmitted energy using a calibrated pyroelectric thermal detector. The calibration transfer was conducted while operating the transmitter in a single-pulsed mode, to avoid thermal detector biases. Results are well correlated between all detectors at lower energy levels. The decrease of the correlation at higher energy levels suggests some saturation effects. In double-pulse mode, PIN and PEM detectors correlate better for the lower off-line energy. In all circumstances PIN detector exhibited higher signal-to-noise ratio than the PEM detector. On the other hand, PEM detector exhibited faster response for better profiling the laser pulse. Radiation intensity sampling should be adjusted to optimize SNR and pulse energy correlation to the actual transmitted energy.

ACKNOWLEGMENT

The authors would like to acknowledge NASA Earth Science Technology Office for the support of this work through funding the 2-μm double-pulse CO_2 IPDA lidar program.

REFERENCES

[1] Menzies, R. and Chahine M., "Remote atmospheric sensing with an airborne laser absorption spectrometer," Applied Optics, 13(12), 2840-2849 (1974).
[2] Ehret, G., Kiemle, C., Wirth, M., Amediek, A., Fix, A. and Houweling, S., "Space-borne remote sensing of CO2, CH4 and N2O by integrated path differential absorption lidar: a sensitivity analysis," Applied Physics B, 90, 593-608 (2008).
[3] Kiemle, C., Quatrevalet, M., Ehret, G., Amediek, A., Fix, A. and Wirth, M., "Sensitivity studies for a space-based methane lidar mission," Atmospheric Measurements Techniques, 4, 2195-2211 (2011).
[4] Refaat, T., Ismail, S., Nehrir, A., Hair, J., Crawford, J., Leifer, I. and Shuman, T., "Performance evaluation of a 1.6-μm methane DIAL system from ground, aircraft and UAV platforms," Optics Express, 21(25), 30415-30432 (2013).
[5] Upendra, S., Yu, J., Petros, M., Refaat, T. and Reithmaier, K., "Development of a pulsed 2-micron integrated path differential absorption lidar for CO_2 measurement," Invited, Proc. SPIE 8872, 887209 (2013).
[6] Yu, J., Petros, M., Reithmaier, K., Bai, Y., Trieu, B., Refaat, T., Kavaya, M., Singh, U. and Ismail, S., "A 2-micron pulsed integrated path differential absorption lidar development for atmospheric CO_2 concentration measurements," 26th International Laser Radar Conference, Porto Heli, Greece (2012).
[7] Yu, J., Trieu, B., Modlin, E., Singh, U. and Kavaya, M., "1 J/ pulse Q-switched 2 μm solid-state laser," Optics Letters, 31(4), 462-464 (2006).
[8] Rogalski, A., [Infrared Detectors], Second Edition, CRC Press, Taylor & Francis Group, New York, (2011).
[9] Gentec-eo, [Product Guide, Laser Beam Measurement], Catalogue, V1.0 (2013).